

Electric field induced localization phenomena in a ladder network with superlattice configuration: Effect of backbone environment

Paramita Dutta,^{1,*} Santanu K. Maiti,^{2,†} and S. N. Karmakar^{1,‡}

¹*Condensed Matter Physics Division, Saha Institute of Nuclear Physics,
Sector-I, Block-AF, Bidhannagar, Kolkata-700 064, India*

²*Physics and Applied Mathematics Unit, Indian Statistical Institute,
203 Barrackpore Trunk Road, Kolkata-700 108, India*

Electric field induced localization properties of a tight-binding ladder network in presence of backbone sites are investigated. Based on Green's function formalism we numerically calculate two-terminal transport together with density of states for different arrangements of atomic sites in the ladder and its backbone. Our results lead to a possibility of getting multiple mobility edges which essentially plays a switching action between a completely opaque to fully or partly conducting region upon the variation of system Fermi energy, and thus, support in fabricating mesoscopic or DNA-based switching devices.

PACS numbers: 73.23.-b, 71.30.+h, 71.23.An, 73.63.Rt

I. INTRODUCTION

Manifestation of localization of single particle states in low-dimensional quantum systems has always been in limelight of research in condensed matter physics since its prediction. Studies on this topic was basically stimulated after the work of Anderson in 1958¹ which has become a milestone in material science. It is well set that exponentially localized states are the only allowed solutions for one-dimensional (1D) systems with random on-site potentials^{1,2}. Apart from the above mentioned fact, another kind of localization phenomenon, the so-called Wannier-Stark localization³, has also drawn much attention of many physicists^{4,5}. This type of localizing behavior is observed in 1D systems subjected to an external electric field, even in absence of any kind of disorder. Although the existence of localized surface states in crystals has been first suggested by Tamm⁶, on the basis of a special 1D model proposed by James⁷, popularity of this phenomenon among scientists has been started to grow following the work of Wannier³ which has won its way after the widespread application to the optical properties of quantum wells^{8,9}.

For both these two typical cases i.e., systems with random site energies and samples with external electric field, one cannot find the existence of *mobility edge* separating the conducting states from the non-conducting region, since all the energy levels are localized. Therefore, for these models no long-range transport will be obtained. However, a large number of physically relevant models are available which exhibit mobility edges at some typical energy values. For example, a 1D tight-binding (TB) chain composed of two uncorrelated random atomic sites exhibits extended energy eigenstates for some specific electron energies over the entire material under a suitable alignment of these random sites as originally explored by Dunlap *et al.*¹⁰. In this case, a short range positional correlation among the atomic sites is established. On the other hand, in quasi-periodic Aubry-Andre model¹¹,

where long range positional correlation is found to exist between the atomic sites in 1D geometry, conducting energy levels are also noticed. All these special classes of materials, the so-called correlated disordered materials, have provided a new turn in the localization phenomena.

Although few attempts^{12–18} have been made to explore the existence of mobility edges in some one- and two-dimensional (2D) systems, a detailed analysis of it is still missing which essentially motivates us to investigate this phenomenon with a renewed interest. In this work we investigate localization properties of a tight-binding ladder network, constructed by coupling two superlattice chains laterally (see Fig.1), in presence of an external electric field. Incidentally, many interesting and novel features of electronic properties have already been examined in different types of 1D superlattice chains^{19–23}, which are considered as the equivalent representation of periodic structures of different metallic layers^{24–26}. The motivation of the present study is two-fold. Firstly, we intend to reveal the interplay of the superlattice configuration in the ladder network and the external electric field on electronic conductance. If the mobility edge phenomenon in such a system still persists at multiple electron energies like a 1D superlattice chain in presence of external electric field, then a ladder network of this particular type, can be used in electronic circuits as a switching device which might throw new light in the present era of nanotechnology. Secondly, the ladder networks are extremely suitable for explaining charge transport through double stranded DNA^{27–29}. A clear understanding of it is highly important due to its potential application in nano-electronics, especially, to design DNA-based computers. Not only that, it has also broad applications in biology since it is directly related to cell division, protein binding processes, etc. Experimental results suggest that DNA can have all possible conducting properties like, metallic³⁰, semiconducting^{31,32} or even insulating^{33,34}. In spite of the numerous experimental and theoretical^{35–37} progress of charge transport through double helix DNA structures,

the conducting nature of DNA molecules are not yet well explained and a deeper analysis is still needed, in the context of fundamental physics and technological interest. Nowadays scientists are trying to develop artificial DNA molecules³⁸, based on DNA synthesis equipment, those are highly stable and analogous to naturally occurred DNA molecules. Therefore, the study of electronic transport in a ladder network comprising of superlattices can give rise significant new results.

To make the present model much more realistic one should consider the effect of backbones and the environment. Though backbone sites are not directly involved on electronic conduction, but the effect of environment can be well analyzed since it essentially tunes the on-site potentials of these sites which results some interesting patterns. In our present work we consider different arrangements of backbone sites (see Fig.1) and consider their effect on electronic conduction, to make it a self-contained study.

The rest of the article is arranged as follows. In Section II we present the model and the calculation method. The numerical results from our model calculations are illustrated in Section III, and finally, in Section IV we summarize the essential results.

II. MODEL AND THEORETICAL FRAMEWORK

Here we present the model quantum system considered for this work and the theoretical formulation to describe electronic transport properties in presence of an external

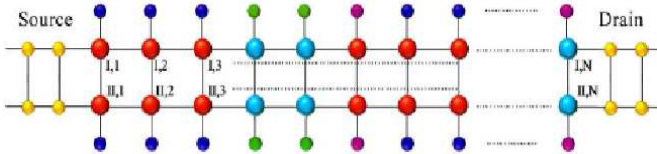


FIG. 1: (Color online). A tight-binding ladder network coupled to finite width source and drain electrodes. The filled circles with different colors correspond to different atomic sites.

bias. We use a simple TB framework to describe the system Hamiltonian, and, within non-interacting picture this approach is highly suitable for analyzing electron transport through a bridge system.

A. The TB model

We consider a conducting junction in which a ladder network is clamped between source and drain electrodes. A sketch of such a source-conductor-drain junction is presented in Fig. 1, where the filled circles with different colors correspond to different atomic sites. The Hamiltonian of this full system can be written as sum of three

terms like,

$$\mathbf{H} = \mathbf{H}_{\text{lad}} + \mathbf{H}_{\text{eltd}} + \mathbf{H}_{\text{tun}}. \quad (1)$$

The first term of Eq. 1 represents the Hamiltonian of the ladder network, while the next two terms correspond to the Hamiltonians of the side attached electrodes and electrode-to-ladder couplings, respectively.

Under nearest-neighbor hopping approximation the TB Hamiltonian of the ladder network in site representation reads as,

$$\begin{aligned} \mathbf{H}_{\text{lad}} = & \sum_{i=I,II} \sum_j \left[\epsilon_{i,j} c_{i,j}^\dagger c_{i,j} + t \left(c_{i,j}^\dagger c_{i,j+1} + \text{h.c.} \right) \right] \\ & + \sum_j v \left(c_{I,j}^\dagger c_{II,j} + c_{II,j}^\dagger c_{I,j} \right) \\ & + \sum_{i=I,II} \sum_j \left[\epsilon_{i,j}^b c_{i,j}^{b\dagger} c_{i,j}^b + t^b \left(c_{i,j}^{b\dagger} c_{i,j}^b + \text{h.c.} \right) \right] \end{aligned} \quad (2)$$

where the index $i(= I, II)$ corresponds to two strands of the ladder and the index $j(= 1, 2, 3, \dots)$ refers to the atomic sites in these strands. Thus, using the notation (i, j) we can locate atomic sites in any strand. Each of these sites is again directly coupled to a backbone site (see Fig. 1) which essentially captures the effect of the environment. $\epsilon_{i,j}$ is the on-site energy of an electron at the site j of i -th strand, and t and v are the intra-strand and inter-strand hopping integrals, respectively. $c_{i,j}^\dagger$ ($c_{i,j}$) is the creation (annihilation) operator of an electron at the site (i, j) . For the backbones we use an additional index b in our TB model to describe the parameters like, on-site energies and hopping matrix elements, such that they are distinguished from the parameters used in the parent ladder. The backbone sites are modeled by the on-site energies $\epsilon_{i,j}^b$, while their couplings to the atomic sites of the strands are characterized by the nearest-neighbor hopping integrals t^b .

Depending on the arrangements of atomic sites in two different strands as well as in backbones, several cases are analyzed to describe the localization phenomena in presence of an external voltage bias. We essentially focus on two different setups. In one case the upper and lower strands are arranged with superlattice configurations, setting the uniform site energies in the backbones, while in the other case the scenario gets reversed. Here, the strands are arranged with identical lattice sites and the backbone sites are configured with superlattice sites. In the present communication, we describe the superlattice models considering two or three types of atoms, in each unit cell, those are labeled as α and β or α, β and γ , and they are arranged following a particular sequence. For example, it can be either $\alpha^p \beta^q$ or $\alpha^p \beta^q \gamma^r$, where p, q and r are three positive integers. Repeating such unit cells we will get the entire lattice chain and construct the desired full system for our study.

In presence of a finite voltage bias V between the source and drain electrodes, an electric field is established

which results the site energies of the bridging conductor voltage dependent. Mathematically it reads as,

$$\epsilon_{i,j} = \epsilon_{i,j}(0) + \epsilon_{i,j}(V) \quad (3)$$

where, $\epsilon_{i,j}(0)$ represents the site energy in absence of external bias V . Depending on the nature of atomic sites $\epsilon_{i,j}(0)$'s are called as $\epsilon_\alpha(0)$, $\epsilon_\beta(0)$, $\epsilon_\gamma(0)$ corresponding to α , β , γ type atomic sites, respectively. The voltage dependence in site energies essentially comes from two regions. One from the bare electric field in the source-

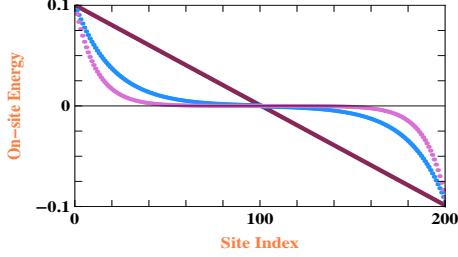


FIG. 2: (Color online). Voltage dependent site energies for three different potential profiles in a 200-rung ladder network when the external bias V is set at 0.2.

conductor-drain bias junctions and the other from the screening in presence of long-range electron-electron (e-e) interactions, which is not directly taken into account in the Hamiltonian Eq. 2. If initially we don't consider the effect of such screening due to e-e interactions, then the electric field becomes uniform along the ladder and it gets the form,

$$\epsilon_{i,j}(V) = V/2 - \frac{jV}{N_r + 1} \quad (4)$$

where, N_r is the total number of rungs in the ladder. Each of these rungs is attached to two backbone sites in opposite sides of the strands ($i = I, II$) whose site energies are also identically modified, following Eq. 4, in presence of voltage bias like the parent lattice sites in individual rungs. Thus, site energies of four atomic sites (two parent and two backbone sites) in each vertical line get equally modified in presence of external bias and their voltage dependence depend only on the distance from the finite width source electrode which results Eq. 4 i independent. Now, if we consider the screening effect, then the electric field will no longer be linear. Two such cases are shown in Fig. 2 for two different screening strengths, as illustrative examples. Below, we will analyze the localization phenomena in the ladder network considering both linear and non-linear bias drops.

The TB Hamiltonians of the finite width electrodes (\mathbf{H}_{eltd}) and electrode-ladder couplings (\mathbf{H}_{tun}) are also expressed quite similar to Eq. 2, where the electrodes are described with on-site energies ϵ_0 and nearest-neighbor interactions t_0 . Two atomic sites of the ladder are directly coupled to the atomic sites of the source electrode where the coupling strength is described by τ_S and it is τ_D for the drain-ladder coupling.

B. Theoretical methods: Green's function approach

To find electronic transmission coefficient for this bridge setup, we use Green's function formalism^{39–41} which is quite robust compared to other existing theories available in literature. In this approach an infinite dimensional system (since electrodes are semi-infinite) gets effectively reduced to the dimension of a finite size conductor clamped between two electrodes.

Using Fisher-Lee relation³⁹, the two-terminal transmission probability can be written as,

$$T = \text{Tr} [\mathbf{\Gamma}_S \mathbf{G}_{\text{lad}}^r \mathbf{\Gamma}_D \mathbf{G}_{\text{lad}}^a] \quad (5)$$

where, $\mathbf{\Gamma}_S$ and $\mathbf{\Gamma}_D$ are the coupling matrices and $\mathbf{G}_{\text{lad}}^r$ and $\mathbf{G}_{\text{lad}}^a$ are the retarded and advanced Green's functions of the ladder network, respectively. The single particle Green's function operator representing the complete system i.e., ladder including source and drain electrodes, for an electron having energy E is defined as,

$$\mathbf{G} = [(E + i\eta)\mathbf{I} - \mathbf{H}]^{-1} \quad (6)$$

where, $\eta \rightarrow 0^+$. \mathbf{H} is the Hamiltonian of the full system and \mathbf{I} denotes the identity matrix. Introducing the concept of self-energies due to source and drain, the problem of finding \mathbf{G} in the full Hilbert space of \mathbf{H} can eventually be mapped to a reduced Hilbert space of the finite ladder, and the effective Green's function $\mathbf{G}_{\text{lad}}^r$ looks like,

$$\mathbf{G}_{\text{lad}}^r = [(E + i\eta)\mathbf{I} - \mathbf{H}_{\text{lad}} - \mathbf{\Sigma}_S^r - \mathbf{\Sigma}_D^r]^{-1}. \quad (7)$$

where, $\mathbf{\Sigma}_S$ and $\mathbf{\Sigma}_D$ are the contact self-energies used to describe the effect of couplings of the ladder to the source and drain, respectively. A detailed derivations of these self-energies are available in Refs.^{40–43}.

The coupling matrices $\mathbf{\Gamma}_S$ and $\mathbf{\Gamma}_D$ corresponding to the couplings of the ladder to the source and drain electrodes are directly associated with the self-energies and they are,

$$\begin{aligned} \mathbf{\Gamma}_{S(D)} &= i [\mathbf{\Sigma}_{S(D)}^r - \mathbf{\Sigma}_{S(D)}^a] \\ &= -2 \text{Im} (\mathbf{\Sigma}_{S(D)}^r). \end{aligned} \quad (8)$$

$\mathbf{\Sigma}_{S(D)}^r$, on the other hand, is the sum $\mathbf{\Sigma}_{S(D)}^r = \mathbf{\Lambda}_{S(D)} + i\mathbf{\Delta}_{S(D)}$, where the real part $\mathbf{\Lambda}_{S(D)}$ corresponds to the shift of energy levels of the ladder, and the imaginary part ($\mathbf{\Delta}_{S(D)}$) is responsible for the broadening of these levels.

Finally, the average density of states (ADOS) of the ladder is determined from the relation,

$$\rho(E) = -\frac{1}{\pi N_s} \text{Im} [\text{Tr} \mathbf{G}_{\text{lad}}^r] \quad (9)$$

where, N_s is the total number of atoms in the ladder network.

III. NUMERICAL RESULTS AND DISCUSSION

In this section, we describe numerical results obtained from the above theoretical prescription given in Section II to investigate localization phenomena in the ladder

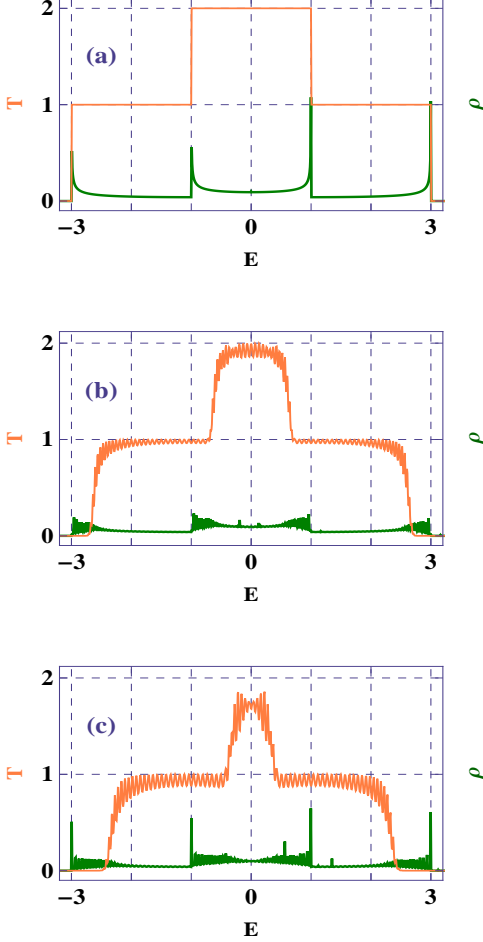


FIG. 3: (Color online). Two-terminal transmission probability T (orange line) as a function of electron energy E for a perfect ladder, in absence of backbone sites, considering the linear potential drop as shown by the red curve in Fig. 2, where (a), (b) and (c) correspond to $V = 0, 0.2$ and 0.4 , respectively. The ADOS (green line) is superimposed in each spectrum. Here we set $N_r = 80$.

network subjected to an external bias. Throughout the analysis we fix the electronic temperature at zero and choose $c = e = \hbar = 1$ for simplification. All the energies are scaled in unit of the hopping integral t .

As stated earlier, two different cases are analyzed depending on the superlattice configurations in the strands and backbones. In one setup, the strands are arranged with superlattice sites considering identical backbone sites, while in the other setup its opposite consequence is taken into account.

Before addressing these central cases, let us first dis-

cuss the effect of voltage bias on electron transport in a simple system which is a perfect ladder without any backbone sites. The results of such a simple model is presented in Fig. 3, where we choose $N_r = 80$. For this ladder, the voltage independent sites energies ($\epsilon_{i,j}(0)$'s) are identical, and therefore, they can be fixed at zero, without any loss of generality. The other parameters used here are as follows. The nearest-neighbor hopping integrals t and v are fixed at 1, and the ladder-electrode coupling constants are taken to be $\tau_S = \tau_D = 1$. In side-attached electrodes, the on-site potentials ϵ_0 and hopping integrals t_0 are set at 0 and 1, respectively. Depending on the potential drop between the source and drain electrodes, three different cases are taken into account those are presented in Figs. 3(a), (b) and (c) where we select $V = 0, 0.2$ and 0.4 , respectively. In each of these three spectra two-terminal transmission probability together with average density of states are shown. All these results are computed considering a linear potential profile along the ladder. In the absence of any electric field associated with the voltage bias, electrons can conduct through the ladder for all possible allowed energies corresponding to the energy eigenvalues of the ladder which can be clearly noticed from the upper panel of Fig. 3(a). Under this condition i.e., $V = 0$, on-site potentials are no longer affected and it results extended energy levels throughout the energy band window of the ordered ladder. The situation becomes somewhat interesting when a finite potential drop appears along the ladder (Figs. 3(b) and (c)). It is observed that several energy levels along the energy band edges do not contribute anything to the electron conduction i.e., transmission coefficient drops to zero for these energies. Obviously, if the Fermi energy of the ladder lies within these regions, no electron transmission takes place and the insulating phase is obtained. The finite transmission will take place only when the energy moves towards the band centre. Thus, a sharp transition between a fully insulating zone to a conducting zone is obtained which gives rise to the phenomenon of mobility edge in presence of external electric field. In presence of a non-zero bias, site energies are voltage dependent (see Eq. 3), those are also not identical to each other, which are responsible for generating localized energy levels in the energy spectrum. Certainly, more such localized energy levels will be available for higher potential drop. This is exactly shown in Fig. 3(c), considering a finite bias $V = 0.4$. It should be noted that, like a conventional disordered material, the localization of energy levels always starts from the band edges, keeping the extended states towards the band centre. This phenomenon has been revisited in our recent work in the context of studying integer quantum Hall effect⁴⁴ within a tight-binding framework. It reveals that, for large enough electric field almost all the energy levels get localized, and therefore, no such crossover between a conducting zone and an insulating phase is observed.

Based on the above analysis of electronic localization in a perfect ladder in presence of external electric field now

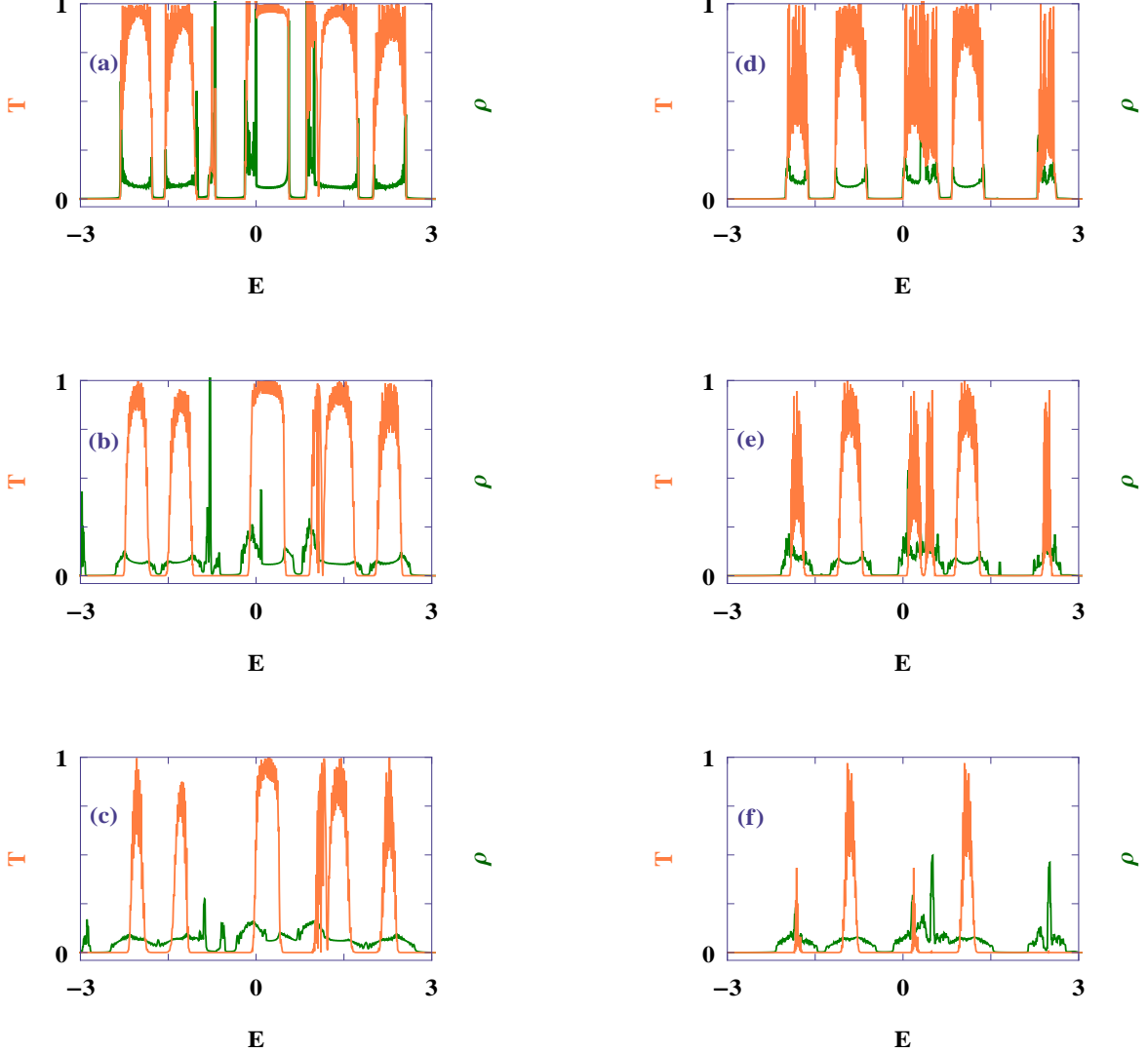


FIG. 4: (Color online). Two-terminal transmission probability T together with average density of states ρ as a function of energy E for a 150-rung ladder network, considering of a linear bias drop along the ladder, where the upper, middle and lower rows correspond to $V = 0, 0.2$ and 0.4 , respectively. Two columns represent two different arrangements of α and β sites. In the left column, the results are computed for the network where we choose $p = 3$ and $q = 2$ in the upper strand, and $p = q = 1$ in the lower strand. While, in the other column we set $p = 3$ and $q = 2$ in both strands. All these results are done for $t^b = 0$. The orange and green lines correspond to the identical meaning as stated in Fig. 3.

we concentrate on the central results i.e., the interplay of superlattice configuration in parent strands as well as in backbones of the ladder network and the external electric field associated with the voltage bias. In what follows, we present our results in two sub-sections for two different setups.

A. The TB ladder network with superlattice chains and identical backbone sites

Here we present our numerical results for the ladder network considering superlattice sites in the strands, set-

ting identical lattice sites in backbones. Two different types of atomic sites, labeled as α and β , are taken into account and depending on their arrangements in the strands several cases are analyzed. These arrangements are specified by the rule $\alpha^p\beta^q$, as stated earlier, where p and q are variables. The parameters used here for the calculations, unless stated otherwise, are $\epsilon_\alpha(0) = -\epsilon_\beta(0) = 1$, $\epsilon_\alpha^b(0) = \epsilon_\beta^b(0) = 0$, $t = v = 1$, $\epsilon_0 = 0$, $t_0 = 1$ and $\tau_S = \tau_D = 1$. The hopping integral t^b is mentioned in the figure captions.

As illustrative examples, in Fig. 4 we present two-terminal transmission probability together with average

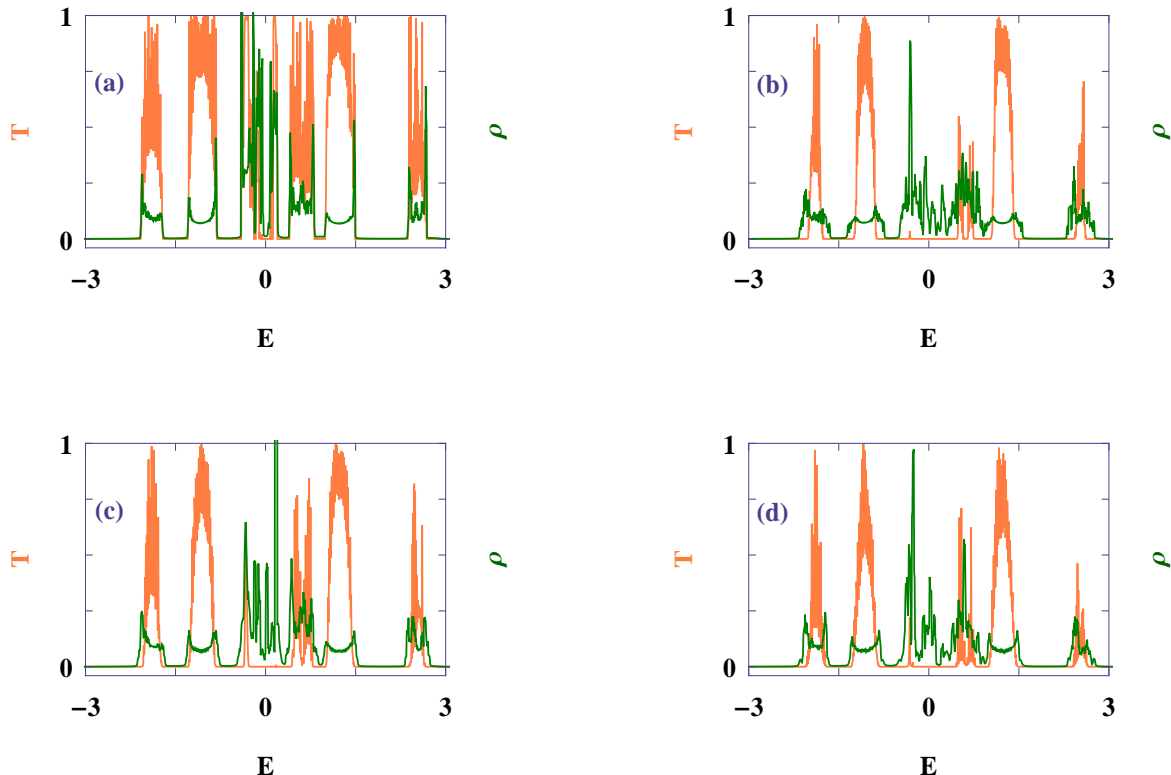


FIG. 5: (Color online). Two-terminal transmission probability and average density of states as a function of energy E for a 150-rung ladder network considering $t^b = 0.4$, where the orange and green curves represent the similar meaning as stated earlier. The results shown in (a) and (b) are computed for a linear potential profile, whereas (c) and (d) are done for the non-linear potential profiles given by the blue and pink lines in Fig. 2, respectively. In (a) we set $V = 0$, while in the other three spectra (c-d) we choose $V = 0.2$. All these results are performed setting $p = 3$ and $q = 2$ in the upper and lower strands of the ladder network.

density of states of a 150-rung ladder network, considering $t^b = 0$ i.e., effect of backbone sites is ignored, for different configurations of α and β sites in two strands. For example, in the left column the results are shown when we choose $p = 3$ and $q = 2$ in the upper strand and these parameters are set equal to 1 for the other strand. On the other hand, in the right column we select $p = 3$ and $q = 2$ for both these two strands. All these results are computed taking a linear potential profile along the ladder. Quite interestingly we see that, in presence of superlattice sites multiple energy bands, separated by finite gaps, are appeared in the energy spectra. Depending on the arrangements of superlattice sites, i.e., the choices of unit cells in two different strands, total number of such energy bands varies. Under this situation when we consider the effect of external electric field associated with the voltage bias, we get multiple localized regions, generated from the band edges, those are separated from the extended energy zones (see the spectra in Fig. 4). Therefore, setting the Fermi energy in suitable energy regions the ladder network can be used to transmit electrons or not from the source to drain electrode, and thus, support in fabricating mesoscopic switching devices at mul-

tiples energies. This essentially leads to the phenomenon of getting multiple mobility edges.

The appearance of energy bands, separated by finite energy gaps, in presence of superlattice sites in the strands is strongly affected by the backbone sites, and the localization properties for a particular configuration, on the other hand, are highly influenced by the nature of electrostatic potential profiles. These issues are addressed in Fig. 5, where we choose $N_r = 180$ and set $p = 3$ and $q = 2$ in both strands of the ladder network. In the upper panel the results are calculated considering a linear bias drop along the sample, while in the lower panel they are computed for non-linear potential profiles. Comparing the spectra shown in Figs. 4(d) and 5(a) (since in these two cases all other parameters, except t^b , are identical) we emphasize that the ADOS spectra can be controlled in a significant way by means of the backbone environment. This change in the density profile becomes much pronounced when the difference between the parameters p and q is quite large, which we justify through our extensive numerical analysis. The effects of backbone sites is elaborately discussed in the following sub-section.

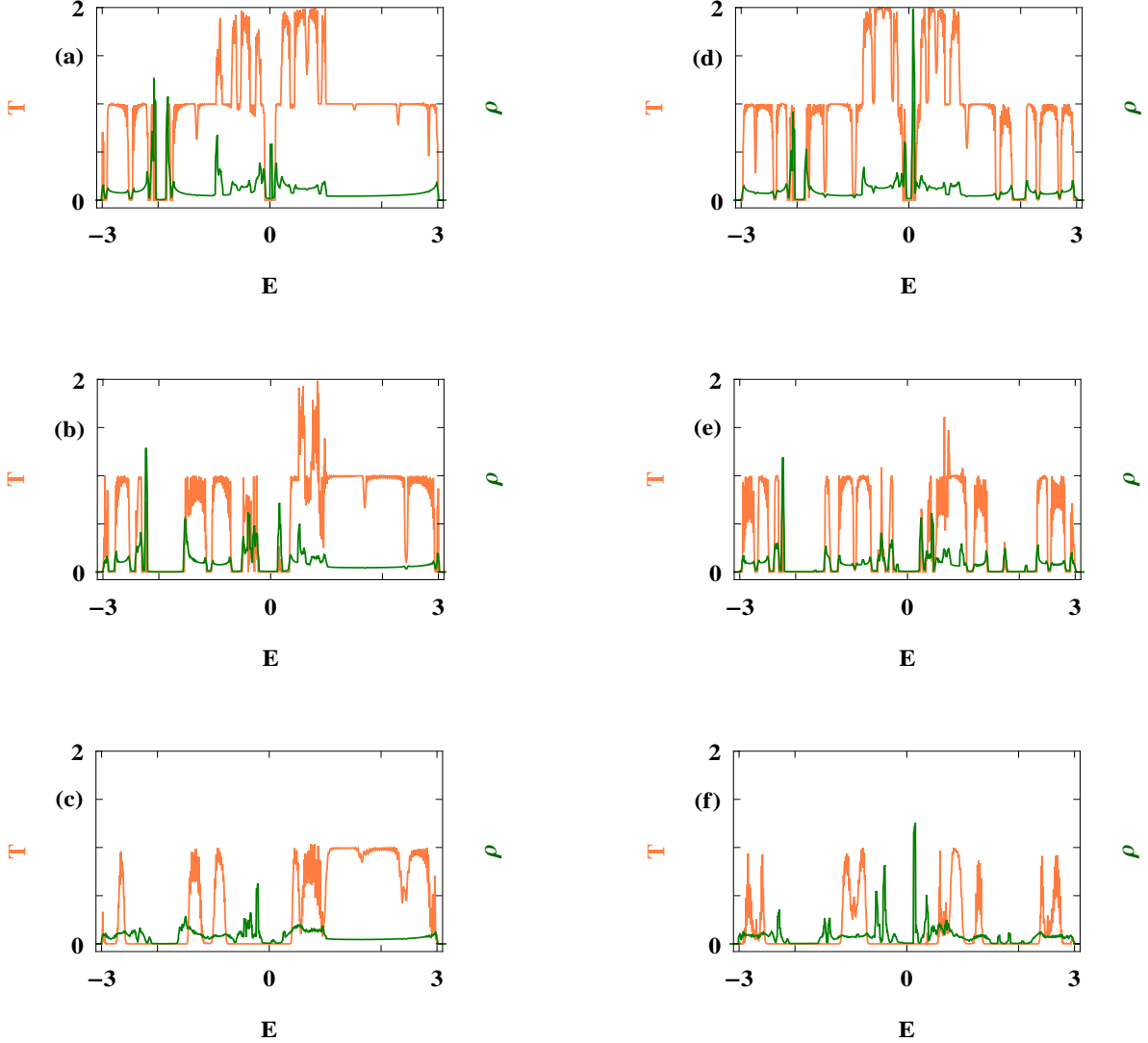


FIG. 6: (Color online). Two-terminal transmission probability T and average density of states ρ as a function of energy E for a ladder network in which strands are arranged with identical lattice sites and the backbones are configured with superlattice sites. In the left column, backbones are arranged with α and β sites where we set $p = 5$ and $q = 2$, while in the right column they are arranged with α , β and γ sites considering $p = 5$, $q = 3$ and $r = 2$. The results given in the 1st row are with $t^b = 0.4$, while all the other results are computed when t^b is fixed at 0.8. The voltage V is taken to be zero in the 1st and 2nd rows, whereas it is 0.2 in the 3rd row. All these results are performed considering a linear electrostatic potential profile. Moreover, we choose total number of rungs $N_r = 140$ for the left column, while it is 150 in the right column. Two different colors correspond to the identical meaning as mentioned in the above figures.

Keeping in mind the possibilities of having much more electron screening now we present the results (Figs. 5(c) and (d)) where non-linear potential profiles are considered. With increasing the flatness of the electrostatic potential profile, the localized regions get decreased. Eventually, for the extreme condition i.e., when the bias drop takes place only at the ladder-to-electrode interfaces no such localized regions will be obtained, and certainly, metal-to-insulator transition cannot be obtained.

So far the results discussed are for the systems where strands are arranged with superlattice configuration.

Now the question is, can one get multiple mobility edges if the backbone sites are modulated with superlattice sites instead of the strands? If yes, then few more advantages are there than the cases studied above. First, one can easily tune backbone site energies by placing the sample in the vicinity of external gate electrodes which can control the band spectra, and thus, results a selective switching action for a fixed Fermi energy in presence of external electric field. Second, the environmental effect on electron transport as present in natural DNA molecules can also be explained through our model quan-

tum systems. Below, these issues are discussed with some typical examples.

B. The TB ladder network with identical lattices in strands and superlattice sites in backbones

Finally, we consider the system where strands are arranged with identical atoms and backbones are arranged with superlattice sites. Some typical cases are analyzed depending on the choices of superlattice sites and the results are presented in Fig. 6. For example, in the left column of Fig. 6 the backbone sites are arranged with two different atomic sites α and β obeying the sequence $\alpha^p\beta^q$, while in the right column three atomic sites α , β and γ are used to construct the backbones following the relation $\alpha^p\beta^q\gamma^r$. The parameters considered for these calculations are: $\epsilon_\alpha(0) = \epsilon_\beta(0) = \epsilon_\gamma(0) = 0$, $\epsilon_\alpha^b(0) = -2$, $\epsilon_\beta^b(0) = 0$, $\epsilon_\gamma^b(0) = 2$, $t = v = 1$, $\epsilon_0 = 0$, $t_0 = 1$ and $\tau_S = \tau_D = 1$. The hopping strength t^b is given in the figure caption. From the spectra (Fig. 6), it is interesting to note that multiple energy bands separated by finite gaps are also obtained here like the cases for the ladders with superlattice strands. At the same time, the gap between the energy bands can be tuned by regulating the coupling strength t^b which may provide additional control parameter for getting selective switching effect at the meso-scale level for multiple energies.

IV. CONCLUDING REMARKS

In the present communication, we address electric field effect associated with the applied voltage bias on localiza-

tion phenomena in a tight-binding ladder network with superlattice configuration. Using Green's function approach we compute two-terminal transmission probability along with average density of states for different arrangements of superlattice sites in the strands as well as in the backbones. Our numerical results exhibit several interesting features which essentially lead to a possibility of using the ladder network as a switching device at multiple energies. This switching action is significantly controlled by many factors like, the nature of electrostatic potential profile, presence of backbone sites, coupling between the backbone sites and the sites in the parent strands, etc. With increasing the flatness of the potential profile, related to screening effects, localized energy regions across the band edges gradually decreases, and, for the typical case when potential drop takes place only at the electrode-ladder interfaces, localized regions disappear, and thus, metal-to-insulator transition cannot be observed upon changing the system Fermi energy. Similarly, the backbone sites are also responsible for controlling the switching action which practically suggest us an experiment towards this direction.

Finally, it is important to state that, although the electronic temperature is fixed at zero throughout the analysis, all these results are still valid in the low-temperature limit. This is due to the fact that the thermal broadening of energy levels is much weaker than the broadening caused by ladder-to-electrode coupling^{40,41,45,46}.

Acknowledgment

Second author is thankful to Prof. A. Nitzan for useful conversations.

* Electronic address: paramita.dutta@saha.ac.in

† Electronic address: santanu.maiti@isical.ac.in

‡ Electronic address: sachindranath.karmakar@saha.ac.in

¹ P. W. Anderson, Phys. Rev. **109**, 1492 (1958).

² S. Das Sarma, S. He, and X. C. Xie, Phys. Rev. Lett. **61**, 2144 (1988).

³ G. H. Wannier, Phys. Rev. **117**, 432 (1960).

⁴ J. R. Borysowicz, Phys. Lett. A **231**, 240 (1997).

⁵ N. Zekri, M. Schreiber, R. Ouasti, R. Bouamrane, and A. Brezini, Z. Phys. B **99**, 381 (1996).

⁶ I. Tamm, Physik Zeits. Sowjetunion **1**, 733 (1932).

⁷ H. M. James, Phys. Rev. **76**, 1611 (1949).

⁸ A. Harwit and J. S. Harris, Appl. Phys. Lett. **50**, 685 (1987).

⁹ B. F. Levine, K. K. Choi, C. G. Bethea, J. Walker, and R. J. Malik, Appl. Phys. Lett. **50**, 1092 (1987).

¹⁰ D. H. Dunlap, H.-L. Wu, and P. Phillips, Phys. Rev. Lett. **65**, 88 (1990).

¹¹ S. Aubry and G. André, in *Group Theoretical Methods in Physics*, Annals of the Israel Physical Society Vol. 3, edited by L. Horwitz and Y. Neeman (American Institute of Physics, New York, 1980), p. 133.

¹² C. M. Soukoulis and E. N. Economou, Phys. Rev. Lett. **48**, 1043 (1982).

¹³ S. Das Sarma, S. He, and X. C. Xie, Phys. Rev. Lett. **61**, 2144 (1988).

¹⁴ M. Johansson and R. Riklund, Phys. Rev. B **42**, 8244 (1990).

¹⁵ A. Eilmes, R. A. Römer, and M. Schreiber, Eur. Phys. J. B **23**, 229 (2001).

¹⁶ S. Sil, S. K. Maiti, and A. Chakrabarti, Phys. Rev. Lett. **101**, 076803 (2008).

¹⁷ S. Sil, S. K. Maiti, and A. Chakrabarti, Phys. Rev. B **78**, 113103 (2008).

¹⁸ S. K. Maiti and A. Nitzan, Phys. Lett. A **377**, 1205 (2013).

¹⁹ T. Paiva and R. R. dos Santos, Phys. Rev. Lett. **76**, 1126 (1996).

²⁰ T. Paiva and R. R. dos Santos, Phys. Rev. B **58**, 9607 (1998).

²¹ T. Paiva and R. R. dos Santos, Phys. Rev. B **62**, 7007 (2000).

²² T. Paiva and R. R. dos Santos, Phys. Rev. B **65**, 153101 (2002).

²³ C.-bo Duan and W.-Z. Wang, J. Phys.: Condens. Matter

- 22**, 345601 (2010).
- ²⁴ B. Heinrich and J. F. Cochran, Adv. Phys. **42**, 523 (1993).
- ²⁵ P. Grünberg, S. Demokritov, A. Fuss, M. Vohl, and J. A. Wolf, J. Appl. Phys. **69**, 4789 (1991).
- ²⁶ S. S. P. Parkin, N. More, and K. P. Roche, Phys. Rev. Lett. **64**, 2304 (1990).
- ²⁷ J. Yi, Phys. Rev. B **68**, 193103 (2003).
- ²⁸ E. Díaz, A. Sedrakyan, D. Sedrakyan, and F. Domínguez-Adame, Phys. Rev. B **75**, 014201 (2007).
- ²⁹ V. Apalkov, J. Berashevich, and T. Chakraborty, J. Chem. Phys. **132**, 085102 (2010).
- ³⁰ A. Rakitin, P. Aich, C. Papadopoulos, Y. Kobzar, A. S. Vedeneev, J. S. Lee, and J. M. Xu, Phys. Rev. Lett. **86**, 3670 (2001).
- ³¹ L. Cai, H. Tabata, and T. Kawai, Appl. Phys. Lett. **77**, 3105 (2000).
- ³² D. Porath, A. Bezryadin, S. D. Vries, and C. Dekkar, Nature (London) **403**, 635 (2000).
- ³³ P. J. de Pablo, F. Moreno-Herrero, J. Colchero, J. G. Herrero, P. Herrero, A. M. Baro, P. Ordeyón, J. M. Solar, and E. Artacho, Phys. Rev. Lett. **85**, 4992 (2000).
- ³⁴ E. Braun, Y. Eichen, U. Sivan, and G. Ben-Yoseph, Nature **391**, 775 (1998).
- ³⁵ Y. A. Berlin, A. L. Burin, and M. A. Ratner, J. Am. Chem. Soc. **123**, 260 (2001).
- ³⁶ G. Cuniberti, L. Craco, D. Porath, and C. Dekker, Phys. Rev. B **65**, 241314(R) (2002).
- ³⁷ S. Roche, Phys. Rev. Lett. **91**, 108101 (2003).
- ³⁸ Y. Doi, J. Chiba, T. Morikawa, and M. Inouye, J. Am. Chem. Soc. **130**, 8762 (2008).
- ³⁹ D. S. Fisher and P. A. Lee, Phys. Rev. B **23**, 6851 (1981).
- ⁴⁰ S. Datta, *Electronic Transport in Mesoscopic Systems*, Cambridge University Press, Cambridge (1997).
- ⁴¹ S. Datta, *Quantum Transport: Atom to Transistor*, Cambridge University Press, Cambridge (2005).
- ⁴² B. K. Nikolić and P. B. Allen, J. Phys.: Condens. Matter **12**, 9629 (2000).
- ⁴³ P. Dutta, S. K. Maiti, and S. N. Karmakar, J. Appl. Phys. **114**, 034306 (2013).
- ⁴⁴ P. Dutta, S. K. Maiti, and S. N. Karmakar, J. Appl. Phys. **112**, 044306 (2012).
- ⁴⁵ P. Dutta, S. K. Maiti, and S. N. Karmakar, Org. Electron. **11**, 1120 (2010).
- ⁴⁶ M. Dey, S. K. Maiti, and S. N. Karmakar, Org. Electron. **12**, 1017 (2011).